

Vilnius University
Faculty of Physics
Laboratory of Atomic and Nuclear Physics

Experiment No. 6

INVESTIGATION OF A GEIGER COUNTER

by Andrius Poškus
(e-mail: andrius.poskus@ff.vu.lt)

2024-04-20

Contents

The aim of the experiment	2
1. Tasks	2
2. Control questions	2
3. The types of ionizing radiation	3
4. Properties of gaseous ionization detectors	4
4.1. A simplified model of an ionization detector	4
4.2. Types of gaseous radiation detectors	4
4.3. Electron avalanche and gas multiplication	5
4.4. Detector geometry and spatial distribution of electric field	6
4.5. Geiger discharge	8
4.6. Construction and fill gas of Geiger counters	10
4.7. Quenching of secondary Geiger discharges	11
4.8. Counting curve of a Geiger counter	12
4.9. Dead time of a Geiger counter and a method of measuring it	13
4.9.1. <i>The concept of the dead time and its underlying physics in the case of a Geiger counter</i>	13
4.9.2. <i>Measuring the dead time of a detector by the method of two sources</i>	14
4.10. Efficiency of a Geiger counter	16
4.10.1. <i>The concepts of absolute or relative efficiency of a detector</i>	16
4.10.2. <i>Underlying physics, typical values, and methods of increasing efficiency of a Geiger counter</i>	17
5. Experimental setup and measurement procedure	19
5.1. Experimental equipment	19
5.2. Measurement procedure	19
5.3. Instruction manual of the Isotrak ratemeter	21
6. Analysis of measurement data	25
7. Linear fitting	27

The aim of the experiment

Measure the Geiger plateau, the counting efficiency of the Geiger counter, and the dead time of the Geiger counter.

1. Tasks

1. Measure and plot the dependence of the counting rate on the detector voltage, locate the plateau in it, measure the length of the plateau and its slope. Compare the results with the typical values.
2. Measure the dead time of the counter by the method of two sources. Compare the result with the typical values.
3. Using a gamma source with known activity, measure the counting efficiency of the counter. Compare the result with the typical values for gamma radiation.

2. Control questions

1. Operating principles of gaseous ionization detectors. The circuit diagram of a gaseous ionization detector in pulse mode.
2. Physical processes in ionization chambers, proportional counter, Geiger counters. The concepts of the electron avalanche and Geiger discharge.
3. Would a Geiger counter operate after changing the voltage polarity? Explain the answer.
4. What are the advantages of using concentric cylindrical electrodes in comparison with parallel planar electrodes?
5. Quenching of secondary discharges. The methods of external quenching and internal quenching (self-quenching).
6. Counting curve of a Geiger counter. The concept of the Geiger plateau.
7. The concept of the dead time of a detector. Correction of the measured counting rate when the dead time is known. Why the dead time is less in the case of internal quenching than in the case of external quenching?
8. The method of two sources for measuring the dead time of a detector.
9. The concept of the counting efficiency of a detector. The method of measuring the efficiency.

Recommended reading:

Knoll G. F. Radiation Detection and Measurement. 3rd Edition. New York: John Wiley & Sons, 2000. p. 159 – 214.

3. The types of ionizing radiation

Ionizing radiation is a flux of subatomic particles (e. g. photons, electrons, positrons, protons, neutrons, nuclei, etc.) that cause ionization of atoms of the medium through which the particles pass. **Ionization** means the removal of electrons from atoms of the medium. In order to remove an electron from an atom, a certain amount of energy must be transferred to the atom. According to the law of conservation of energy, this amount of energy is equal to the decrease of kinetic energy of the particle that causes ionization. Therefore, ionization becomes possible only when the energy of incident particles (or of the secondary particles that may appear as a result of interactions of incident particles with matter) exceeds a certain threshold value – the **ionization energy** of the atom. The ionization energy is usually of the order of 10 eV ($1 \text{ eV} = 1,6022 \cdot 10^{-19} \text{ J}$).

Ionizing radiation may be of various nature. The **directly ionizing radiation** is composed of high-energy charged particles, which ionize atoms of the material due to Coulomb interaction with their electrons. Such particles are, e. g., high-energy electrons and positrons (beta radiation), high-energy ^4He nuclei (alpha radiation), various other nuclei. **Indirectly ionizing radiation** is composed of neutral particles which do not directly ionize atoms or do that very infrequently, but due to interactions of those particles with matter high-energy free charged particles are occasionally emitted. The latter particles directly ionize atoms of the medium. Examples of indirectly ionizing radiation are high-energy photons (ultraviolet, X-ray and gamma radiation) and neutrons of any energy. Particle energies of various types of ionizing radiation are given in the two tables below.

Table 1. The scale of wavelengths of electromagnetic radiation

Spectral region	Approximate wavelength range	Approximate range of photon energies
Radio waves	100000 km – 1 mm	$1 \cdot 10^{-14} \text{ eV}$ – 0,001 eV
Infrared rays	1 mm – 0,75 μm	0,001 eV – 1,7 eV
Visible light	0,75 μm – 0,4 μm	1,7 eV – 3,1 eV
Ionizing electromagnetic radiation:		
Ultraviolet light	0,4 μm – 10 nm	3,1 eV – 100 eV
X-ray radiation	10 nm – 0,001 nm	100 eV – 1 MeV
Gamma radiation	< 0,1 nm	> 10 keV

Table 2. Particle energies corresponding to ionizing radiation composed of particles of matter

Radiation type	Approximate range of particle energies
Alpha (α) particles (^4He nuclei)	4 MeV – 9 MeV
Beta (β) particles (electrons and positrons)	10 keV – 10 MeV
Thermal neutrons	< 0,4 eV
Intermediate neutrons	0,4 eV – 200 keV
Fast neutrons	> 200 keV
Nuclear fragments and recoil nuclei	1 MeV – 100 MeV

The mechanism of interaction of particles with matter depends on the nature of the particles (especially on their mass and electric charge). According to the manner by which particles interact with matter, four distinct groups of particles can be defined:

- 1) heavy charged particles (such as alpha particles and nuclei),
- 2) light charged particles (such as electrons and positrons),
- 3) photons (quanta of electromagnetic radiation, which are neutral particles with zero rest mass),
- 4) neutrons (neutral heavy particles).

This experiment concerns only the third mentioned type of particles (photons). However, the physical processes that take place inside a Geiger-Müller tube (the sensing element of a Geiger counter) are essentially the same in the case of any type of radiation detected by the Geiger counter.

4. Properties of gaseous ionization detectors

4.1. A simplified model of an ionization detector

An *ionization detector* is a device for detecting ionizing radiation and for transforming its energy into energy of other types (for example, electric current), which can be easily measured. In order to detect radiation, it must interact with the active medium of the detector. The types of this interaction and its physical mechanisms depend on the nature of the incident radiation and on the energy of its particles. Detectors of different types are sensitive to different types of interaction. As reflected in the name of ionizing radiation, a common outcome of an elementary interaction event is ionization of an atom, i.e., liberation of an electron from it. This event creates at least one free charged particle (electron). The atom that has lost the electron becomes a positive ion, which may also be free, in which case two free charged particles (electron and ion) would be created. Consequently, the simplest principle of operation of an ionization detector is the following:

- (1) radiation creates free charge carriers in the active medium of the detector,
- (2) those charge carriers are accelerated by an external electric field and create electric current in the external circuit.

Thus, a detector may be modeled as a current source, which generates a pulse of electric current $i(t)$ every time when a particle interacts with the active medium (for example, gas or semiconductor) of the detector. The amplitudes (heights) and durations (widths) of different pulses may be different, depending on particular interaction events that caused those pulses (see Fig. 1). Time intervals between pulses are random, because particles interact with the detector at random moments of time.

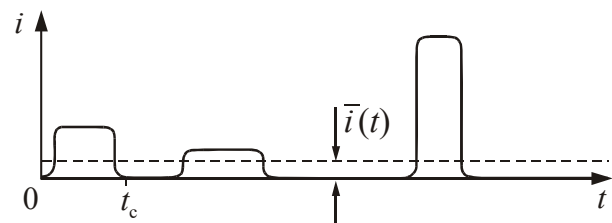


Fig. 1. Examples of current pulses of a detector. The dashed line represents the time average $\bar{i}(t)$.

The two main modes of operation of radiation detectors are called “pulse mode” and “current mode”. In *pulse mode*, the devices that are connected to the detector are designed to register *each* current pulse generated by the detector. This mode is always applied when measuring particle energies (*radiation spectroscopy*). Detectors used in radiation spectroscopy are designed so that the time integral of each current pulse is approximately proportional to particle energy absorbed by the active medium of the detector. This property makes it possible to measure energy of each particle that was absorbed in the detector. Another type of measurements requiring the pulse mode is *particle counting*. In this case, the shape of individual pulses is not important (and their height or time integral is not required to correlate with the absorbed energy); the only thing needed is a sufficiently large pulse height, so that it is easy to count the pulses. For example, particle counting must be performed when measuring activity of a radioactive sample (*activity* is the average number of nuclei that decay per unit time, or the number of particles emitted per unit time).

When the frequency of interaction events in the active medium of the detector is especially high, it may be too difficult to implement the pulse mode, because the time intervals between current pulses may become too small to distinguish one pulse from another, or adjacent pulses may overlap. In such cases, the *current mode* is used, when only the average current is measured (the time averaging interval is assumed to be much greater than the average interval between interaction events). The current mode is also used in most dosimeters, because the absorbed dose of radiation during a particular period of time depends only on the *total* energy absorbed during that time, so that it is sufficient to measure only the total time integral of the current (i.e., its time average multiplied by the time of the exposure to radiation). In Fig. 1, the mentioned time average of the current is shown by the horizontal dashed line.

4.2. Types of gaseous radiation detectors

In gaseous detectors, the active medium is an inert (noble) gas (usually with addition of up to 10 % of another gas), and the mentioned free charge carriers are always created in pairs: electron is created together with a corresponding positive ion. This pair of electron and positive ion is usually called

an *ion pair*. The height and shape of current pulses generated by a gaseous ionization detector depend on electric field strength and its spatial distribution inside the detector. In the case of weak electric field, all ion pairs are *directly* created by the incident particle (i.e., there is no further multiplication of charge carriers due to secondary effects after absorbing all or part of the incident particle energy). In such a case, the number of charge carriers reaching the electrodes per unit time (i.e., the electric current) does not depend on applied voltage and is equal to the number ion pairs created per unit time (assuming that recombination of positive and negative charge carriers is negligible). This is the normal mode of operation of *ionization chambers*. Ionization chambers usually operate in current mode, but they can also operate in pulse mode. At stronger electric fields, electrons can be accelerated to energies greater than the *ionization energy* of gas molecules (this is the minimum energy required to remove the most loosely bound electron of an isolated gas molecule). As a result, *secondary ionization* (also called *impact ionization*) becomes possible: each electron can “knock out” additional electrons from neutral molecules of the gas. Thus, additional ion pairs are created and the amplitude of the current pulse increases. This effect is called *gas multiplication*. Under certain conditions, the gas multiplication factor is approximately constant, i.e., the final number of ion pairs (and the pulse amplitude) is proportional to the number of primary ion pairs (which were directly created by the incident particle). Such gaseous detectors are therefore called *proportional counters*. At especially strong electric fields, even a single ion pair triggers a discharge that propagates over the entire length of the counter tube, and the mentioned proportionality is disrupted: the pulse amplitude stops depending on the number of primary ion pairs and depends only on the applied voltage. The gaseous detectors of the latter type are called *Geiger counters* or *Geiger-Müller counters*, or *G-M counters*. They are named after Hans Geiger, who invented the principle in 1908, and Walther Müller, who collaborated with Geiger in developing the technique further in 1928.

4.3. Electron avalanche and gas multiplication

As the electrons drift towards the positive electrode (anode) and the ions drift towards the negative electrode (cathode), they collide with neutral molecules of the gas many times. During the time interval between each two collisions, both an electron and an ion acquire some kinetic energy from the electric field that exists inside the counter. Ions lose a large part of that additional energy during each collision. This follows from the laws of conservation of energy and momentum: an elastic collision between two particles of almost equal mass (such as an ion and a neutral molecule) usually causes a large exchange of kinetic energy between them, so that the kinetic energy of the faster particle (ion) is efficiently transferred to the slower one (neutral molecule). Consequently, the effect of electric field on the average kinetic energy of an ion is relatively small, and the mentioned energy is always of the order of average thermal energy, i.e., $k_B T$, where k_B is the Boltzmann constant and T is the absolute temperature. At room temperature, $k_B T$ is approximately 0.025 eV, which is much less than the typical ionization energies of gases (10 – 25 eV). Ions therefore cannot cause secondary ionization. On the other hand, an electron loses only a very small fraction of its kinetic energy in an elastic collision with a gas molecule, because the mass of a molecule is greater than the electron mass by 4 or 5 orders of magnitude (an elastic collision with a molecule may cause a large change of electron’s *direction*, but not of its *energy*). As a result, if all collisions were elastic, then kinetic energy of an electron would increase as it approaches anode, and it would eventually exceed the ionization energy. Then the secondary ionization becomes possible: the electron knocks out another electron from a neutral molecule, i.e., creates an additional ion pair, losing most of its kinetic energy in the process.

However, inelastic collisions without ionization are also possible. Those are the collisions when an electron excites a molecule, i.e., increases its internal energy without knocking out another electron. Since probability of an inelastic collision increases with electron energy, a dynamic equilibrium is eventually established, when the average energy lost to inelastic collisions per unit time is equal to the average energy gained due to acceleration by the electric field per unit time. Then the average kinetic of an electron stays approximately constant, and this energy may be insufficient for secondary ionization if the electric field is not sufficiently strong. The average kinetic energy of an electron in a gaseous ionization detector under conditions of a strong electric field is approximately proportional to E / p , where E is the electric field strength, and p is the gas pressure. The “threshold” value of the ratio E / p , which must be exceeded in order for the secondary ionization to become possible, depends on the gas composition. For a typical gas, this threshold ratio is approximately equal to 10 V/(m·Pa). At normal atmospheric pressure ($p \approx 10^5$ Pa), this corresponds to “threshold” electric field strength $E_{\text{ion}} = 10^6$ V/m.

Scattering of the electrons by gas molecules causes frequent random changes in the direction of motion of each electron. If electric field strength is much less than E_{ion} , then motion of electrons is mostly random: at each moment of time, the number of electrons moving towards the anode is only slightly greater than the number of electrons moving in the opposite direction. In other words, the average electron *velocity* (i.e., the “drift” speed, which is equal to the average component of the velocity vector that is parallel to the accelerating force) is significantly less than the average *speed* (i.e., the average absolute value of the velocity vector, disregarding its direction). Consequently, the mentioned increase of average kinetic energy of an electron due to acceleration in electric field may be described as “heating” of the electron gas by the electric field (the term “heating” emphasizes the random character of electron motion). This also means that electrons may be described by an “effective” absolute temperature T_e such that $k_B T_e$ is equal to the average kinetic energy of an electron. Even at electric fields of the order of E_{ion} or greater, the random component in the direction of motion of each electron is still significant (i.e., large changes of electron’s direction due to collisions with gas molecules are still possible). In strong electric field, T_e may exceed the ambient absolute temperature T by two or three orders of magnitude. As mentioned, $k_B T_e$ is proportional to E / p .

The electrons ejected from neutral molecules due to secondary ionization (the “secondary electrons”) are also accelerated by the electric field. As a result, they can also ionize gas molecules, so that a chain reaction becomes possible (see Fig. 2). This chain reaction is called *electron avalanche* or *Townsend discharge*, after the Irish physicist John Sealy Townsend, who discovered this effect in his work between 1897 and 1901. If the total number of free electrons is denoted N , then its relative increase (dN / N) over the infinitesimal distance dx is given by the *Townsend equation*:

$$dP \equiv \frac{dN}{N} = \Sigma dx = \frac{dx}{l_{\text{ion}}}, \quad (4.3.1)$$

where dP is the probability of the secondary ionization over the distance dx , and Σ is the *first Townsend coefficient*, which is equal to the inverse average path of the electron between two secondary ionization events (l_{ion}). Σ is equal to zero when the electric field strength is less than the mentioned threshold value E_{ion} , and it increases with electric field strength (see Fig. 3). In the case of a homogeneous electric field (as in a parallel-plate capacitor), Σ is constant, and the solution of the Townsend equation (4.3.1) is an exponential function:

$$N(x) = N(0)e^{\Sigma x} = N(0)e^{x/l_{\text{ion}}}, \quad (4.3.2)$$

where $N(0)$ is the number of electrons at the point $x = 0$. If electric field is inhomogeneous, then a more general equation must be used instead of (4.3.2):

$$N(x) = N(0)\exp\left(\int_0^x \Sigma(E(x))dx\right), \quad (4.3.3)$$

where $E(x)$ is the electric field strength at the point x . Because of the exponential factor in Eq. (4.3.2) or (4.3.3), the total number of ion pairs (i.e., free electrons) created in the gas may exceed the number of primary ion pairs by a factor of 10^4 or greater. This effect is called *gas multiplication*. It is characterized by the *gas multiplication factor* K , which is defined as the ratio of the total number of ion pairs to the number of primary ion pairs. Gas multiplication is useful, because it causes an increase of the number of charge carriers that reach electrodes of the detector and thus an increase of the detector output pulse amplitude, so that it becomes easier to measure.

4.4. Detector geometry and spatial distribution of electric field

The threshold electric field strength E_{ion} , which must be exceeded in order for the secondary ionization to become possible, can be calculated as follows. The force acting on an electron in electric field is equal to eE , where e is the elementary charge (i.e., the absolute value of the electron charge), and

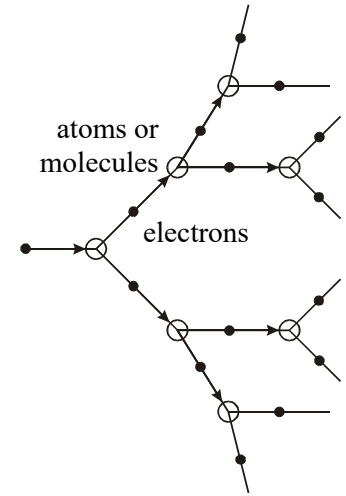


Fig. 2. Electron avalanche

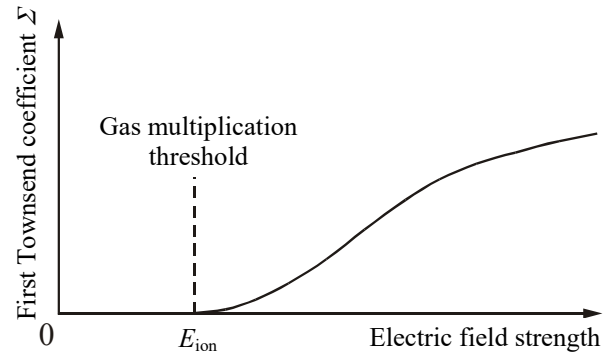


Fig 3. Typical dependence of the first Townsend coefficient on electric field strength

E is the electric field strength. The work done by this force as the electron travels distance x in the direction of the force is equal to xeE . This work is equal to the electron's kinetic energy gained over the distance x . Most of this energy is lost during inelastic collisions of the electron with gas molecules. In order to simplify the calculations, let us assume that the electron does not lose any energy during elastic collisions and loses *all* energy in *each* inelastic collision. Then the average kinetic energy of the electron is equal to the average work done by the accelerating force between two inelastic collisions, i.e., to leE , where l is the average displacement of the electron (in the direction of the accelerating force) between two inelastic collisions. The secondary ionization becomes possible when the mentioned work becomes equal to the ionization energy W_{ion} of a gas molecule. Consequently, the threshold electric field is equal to

$$E_{\text{ion}} = \frac{W_{\text{ion}}}{le}. \quad (4.4.1)$$

A typical value of W_{ion} is 15 eV. A typical value of l at atmospheric pressure (i.e., at 10^5 Pa) is 10^{-5} m. By substituting those two values into Eq. (4.4.1), a value of E_{ion} equal to 1.5×10^6 V/m is obtained. In a parallel-plate capacitor with inter-electrode distance of 1 cm, this would correspond to voltage of 15 kV. Using such a high voltage in a gaseous radiation detector would be inconvenient. However, in the case of a cylindrical detector, where one of the electrodes is a thin wire (see Fig. 4), electric field of the order of 10^6 V/m (at least in a small part of the active volume of the detector) can be achieved at voltages of the order of 100 V. This is because the radial dependence of electric field strength in a cylindrical detector is given by the following equation:

$$E(r) = \frac{U_0}{r \ln \frac{r_c}{r_a}}, \quad (4.4.2)$$

where U_0 is the voltage between the inner and outer electrodes, r is the distance to the symmetry axis of the detector, r_c is the radius of the outer electrode (cathode), and r_a is the radius of the wire acting as the inner electrode (anode). Thus, electric field strength is inversely proportional to r . Consequently, even when U_0 is only a few hundred volts, electric field strength of the order of 10^6 V/m can be achieved at $r \approx 0.1$ mm or less (this implies that r_a is less than 0.1 mm). Thus, the gas multiplication is possible only in a very small volume around the anode. However, since the number of secondary electrons grows exponentially as the avalanche develops (see Eq. (4.3.3)), the majority of secondary electrons is created in a much thinner layer (see Fig. 6), whose thickness ($r' - r_a$) is of the same order of magnitude as the mean path of an electron between two secondary ionization events (a few micrometers).

The especially strong electric field near the thin central anode (see Eq. (4.4.2)) is the main reason why cylindrical electrode arrangement shown in Fig. 4 is always used in Geiger counters. The sensing element of each Geiger counter (called a **Geiger-Müller tube** or **G-M tube**) is a chamber filled with a gas mixture and containing the two electrodes, between which there is a potential difference of several hundred volts.

It should be noted that Eq. (4.4.2) assumes negligible space charge density inside the gas volume ($r_a < r < r_c$). Under certain conditions, this assumption is not true (see Section 4.5).

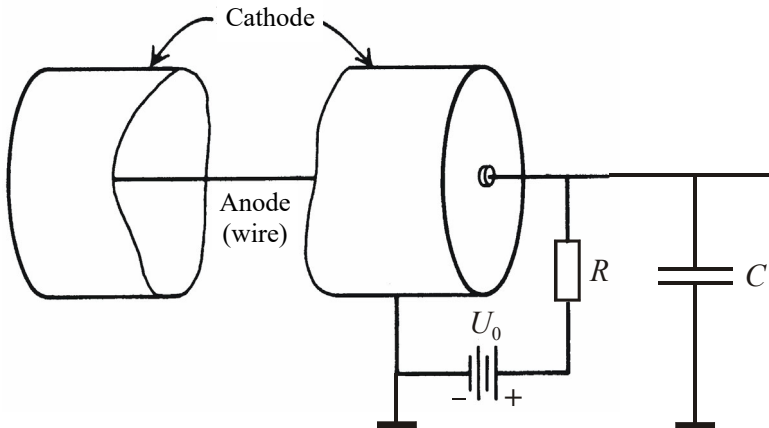


Fig. 4. Main components of a Geiger counter (or proportional counter). The sensing element is a cylindrical Geiger-Müller tube. The output voltage pulse is formed in the load resistor R . C is the sum of the G-M tube anode capacitance and the external equipment capacitance.

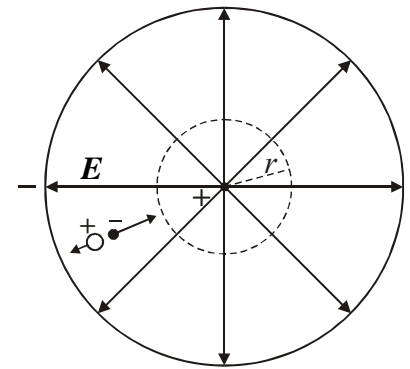


Fig. 5. Cross-section of a cylindrical gaseous radiation detector, and the electric field lines

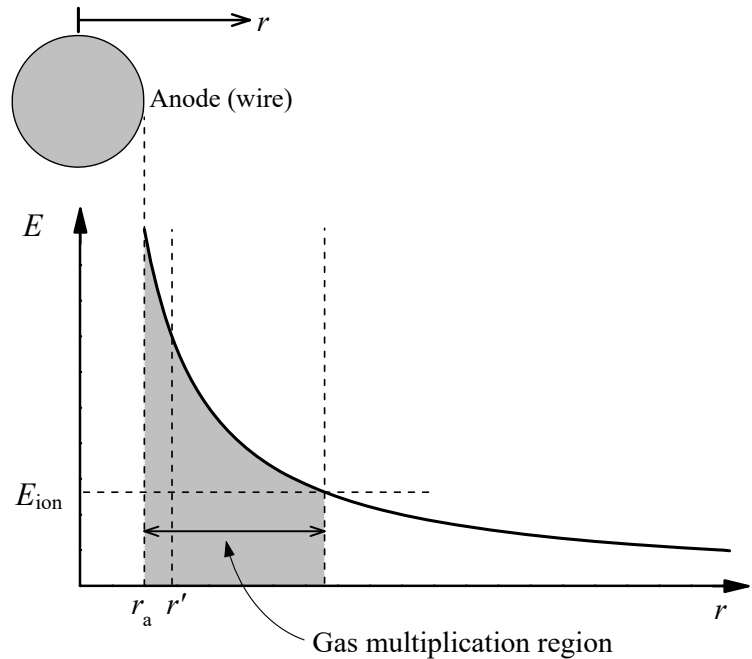


Fig. 6. Radial dependence of electric field strength in a cylindrical gaseous radiation detector. The shaded area corresponds to the volume where the gas multiplication is possible. However, the majority of secondary electrons are created in a much thinner layer from r_a to r' . The value of $r' - r_a$ is of the same order of magnitude as the mean path of an electron between two secondary ionization events (a few micrometers).

4.5. Geiger discharge

As mentioned, inelastic collisions of fast electrons with neutral gas molecules not only cause ionization, but also create molecules and molecular ions with excess internal energy (i.e., *excited* molecules and ions). An excited molecule eventually undergoes a spontaneous quantum transition to a lower energy level (the typical lifetime of an excited molecule is $10^{-9} - 10^{-8}$ s). During this transition, the excess energy is emitted in the form of a quantum of electromagnetic radiation (called a *photon*). On the scale of wavelengths of electromagnetic radiation (see Table 1), the radiation emitted by excited molecules belongs to the ultraviolet spectrum. The corresponding photon energy is of the order of a few electronvolts. Those photons may travel up to several centimeters in the gas before interacting with another gas molecule or reaching the cathode. When a photon of ultraviolet light is absorbed by a gas molecule or by the cathode, an electron may be knocked out of the gas molecule or the cathode. If a photon knocks out an electron from an atom or molecule, then this process is called **photoionization**. If a photon knocks out an electron from the surface of a metal (such as the cathode of a detector), then this process is called **photoelectric effect** or **photoeffect**. In order for the photoionization to be possible, the photon energy must be greater than the ionization energy of the atom or molecule. Similarly, in order for the photoeffect to be possible, the photon energy must be greater than the **work function** of the metal (this term refers to the minimum energy required to remove an electron from the surface of the material). Work functions of most metals are (4–5) eV. The free electrons emitted as a result of photoeffect and photoionization are called **photoelectrons**. Photoelectrons may also ionize gas molecules and thus initiate additional electron avalanches. Those avalanches will be further called “secondary” avalanches. The process of creation of secondary avalanches is illustrated in Fig. 7.

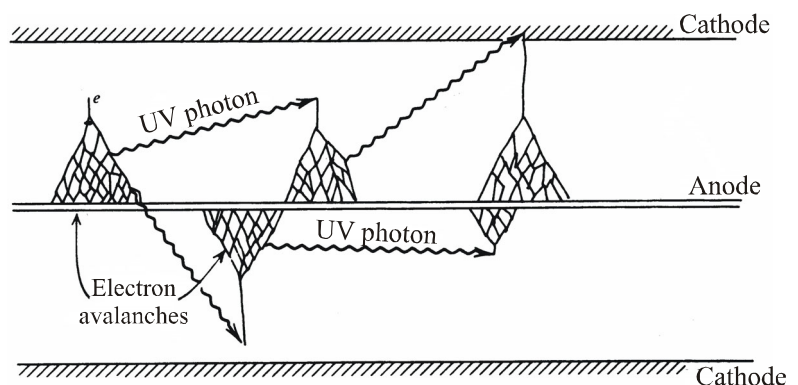


Fig. 7. The process of creation of secondary electron avalanches during a Geiger discharge. Wavy arrows represent photons of ultraviolet light.

Thus, photoelectrons cause an increase of the output voltage pulse of a detector. We will now examine the dependence of the gas multiplication factor on probability of photoelectron emission. Let K denote the gas multiplication factor in absence of photoelectrons. I.e., if there is no photoionization or photoeffect, then each primary electron will create an avalanche consisting of K electrons. Let γ denote

the average number of photoelectrons created by each of those K electrons as they travel towards the anode. Each of those photoelectrons initiates a secondary avalanche. Consequently, a single primary avalanche creates $K\gamma$ secondary avalanches. Since each secondary avalanche also consists of K electrons, the total number of electrons becomes equal to $K + K^2\gamma$. However, the same reasoning can be applied to each secondary avalanche, too. The total number of electrons must therefore be corrected again: $K + K\gamma(K + K^2\gamma) = K + K^2\gamma + K^3\gamma^2$. It follows that the expression of the gas multiplication factor, which takes into account the photoionization and photoeffect, is equal to a sum of a geometric progression:

$$K_{\text{ph}} = K + K^2\gamma + K^3\gamma^2 + \dots = \frac{K}{1 - K\gamma}, \quad (4.5.1)$$

where K_{ph} denotes the gas multiplication factor in presence of photoionization and photoeffect. As it is evident from Eq. (4.5.1), K_{ph} may be much greater than K , depending on γ . In proportional counters, $K\gamma \ll 1$. This means that photoelectrons do not play an important role in proportional counters ($K_{\text{ph}} \approx K$).

If the voltage between the anode and the cathode is increased, then the values of K and γ increase, too. As it follows from Eq. (4.5.1), the increase of K_{ph} is faster than the increase of K . When $K\gamma = 1$, K_{ph} diverges (i.e., becomes infinite). In practice, this means that the entire gas multiplication region surrounding the anode is rapidly filled with a large number of secondary electron avalanches. This is the **Geiger discharge**, which is used in Geiger counters. The electron avalanches propagate along the anode until filling the entire volume with electric field strength greater than the threshold value E_{ion} . As mentioned, the majority of ion pairs are created at a distance of just a few micrometers from the anode (see Fig. 6). Thus, the electron avalanches comprising the Geiger discharge are mostly concentrated inside a cylindrical layer with thickness of a few micrometers adjacent to the anode. The speed of propagation of avalanches is $(2 - 4) \times 10^4$ m/s. Since the length of a typical G-M tube is equal to a few centimeters, all free charge carriers are created during a few microseconds since creation of primary ion pairs.

The discussion above was based on the assumption that the average number of secondary electrons (not counting the photoelectrons) created by a single primary electron (i.e., the gas multiplication factor K) is a constant. This assumption is not correct. As mentioned in Section 4.3, K depends on electric field strength, which, in turn, depends on the space charge density between the electrodes. Most of the secondary electrons and photoelectrons emitted during the Geiger discharge reach the anode in just a few nanoseconds (due to proximity of the electron avalanches to the anode and due to high speed of the electrons). During this short time, the much slower ions practically do not change their positions. This means that positive space charge of the ions builds up around the anode. This “cloud” of positive charge induces an additional opposite negative charge in the (positive) anode. The direction of the additional electric field created by the mentioned induced charge in the anode is opposite to the direction of the total electric field. Consequently, the total electric field near the surface of the anode is reduced. This reduction of electric field strength increases as the Geiger discharge develops (due to the increase of the mentioned positive space charge density), causing a decrease of the gas multiplication factor K , and electron avalanches eventually stop due to insufficient electric field strength. Thus, the total number of electrons that reach the anode depends only on amount of the positive charge needed to stop the Geiger discharge, and does not depend on the number of primary ion pairs. This explains why the amplitude of the output voltage pulse of a Geiger counter does not depend on the primary ionization (unlike in proportional counters). The mentioned amplitude depends on the geometry of the Geiger counter and is approximately proportional to the applied voltage U_0 . However, if primary ion pairs are created at a moment of time when electric field strength has not yet reached the maximum value after the previous Geiger discharge, then a pulse with reduced amplitude will be generated.

As the ions drift towards the cathode, the additional charge induced in the anode and the strength of the corresponding additional electric field decrease, so that the total electric field strength and the gas multiplication factor start to increase again. If free electrons are present inside the detector at the moment of time when K becomes sufficiently large for a Geiger discharge, then another Geiger discharge will develop, causing another voltage pulse. If the mentioned free electrons are a byproduct of the previous Geiger discharge (rather than of another ionizing particle entering the detector from outside), then the corresponding pulse would be a “false” one. Consequently, special measures must be taken in order to eliminate these “secondary” Geiger discharges. This is achieved by ensuring that no additional electrons are emitted during the processes that accompany the dissipation of the positive ion cloud. The main process that may cause emission of additional electrons is neutralization of positive ions as they reach the

cathode. Consequently, the time interval between the primary and secondary Geiger discharge is approximately equal to the time needed for the positive ions to reach the cathode (several milliseconds or longer). The elimination of the secondary Geiger discharges is called “quenching”. The methods of quenching will be described in Section 4.7.

In summary of this section, each Geiger discharge consists of a multitude of electron avalanches, the majority of which are “secondary” avalanches (meaning that they were initiated by photoelectrons). This is true both for the “primary” Geiger discharge and for “secondary” Geiger discharges, which may occur due to neutralization of positive ions at the cathode. Thus, the term “Geiger discharge” should not be confused with the term “electron avalanche” or “Townsend discharge” (in particular, secondary Geiger discharges should not be confused with secondary avalanches).

4.6. Construction and fill gas of Geiger counters

The simplified circuit diagram of a Geiger counter is shown in Fig. 4 (in Section 4.4). The output voltage pulse is formed in the load resistance R . This resistance together with capacitance C forms an equivalent parallel RC circuit representing the equipment that is connected to the G-M tube. This RC circuit converts the *current* pulse generated by the G-M tube into a *voltage* pulse, which is subsequently processed by the external equipment.

As it follows from the principle of operation of a Geiger counter (see Sections 4.3 – 4.5), neutral molecules of the gas filling the G-M tube must not capture free electrons (forming negative ions), because an ion (either positive or negative) cannot initiate an electron avalanche due to the large mass of the ion (see Section 4.3). The main component of the fill gas of a G-M tube is usually a noble gas (for example, argon or helium), because molecules of noble gases are characterized by exceptionally small electron capture cross sections. In addition, the gas mixture usually contains a smaller amount of the second component, which is needed for quenching of secondary Geiger discharges (the methods of quenching will be described in Section 4.7). As mentioned in Section 4.3, there is a certain threshold value of the ratio E/p (where E is the electric field strength near the anode, and p is the gas pressure), which must be exceeded for the secondary ionization to become possible. In order to reduce the corresponding threshold value of E , the gas pressure is usually less than the normal atmospheric pressure (typically by a factor of 3 to 10).

The anode of a G-M tube is usually made of tungsten wire. The cathode is a part of the outer shell of the G-M tube. The cathode may be a thin conductive layer (copper, tungsten, steel, etc.) deposited on the inner surface of a glass tube.

There are two main types of G-M tube construction:

1) **End-window** type G-M tubes have a thin mica window (whose thickness is usually about $10\ \mu\text{m}$) at one end (see Fig. 8a). This thin entrance window is needed to improve sensitivity of the G-M tube to particles with low penetration depth, such as alpha particles (nuclei of ^4He) and low-energy beta particles (electrons or positrons with energy of the order of 10 keV or less), which cannot penetrate the outer electrode (cathode), but

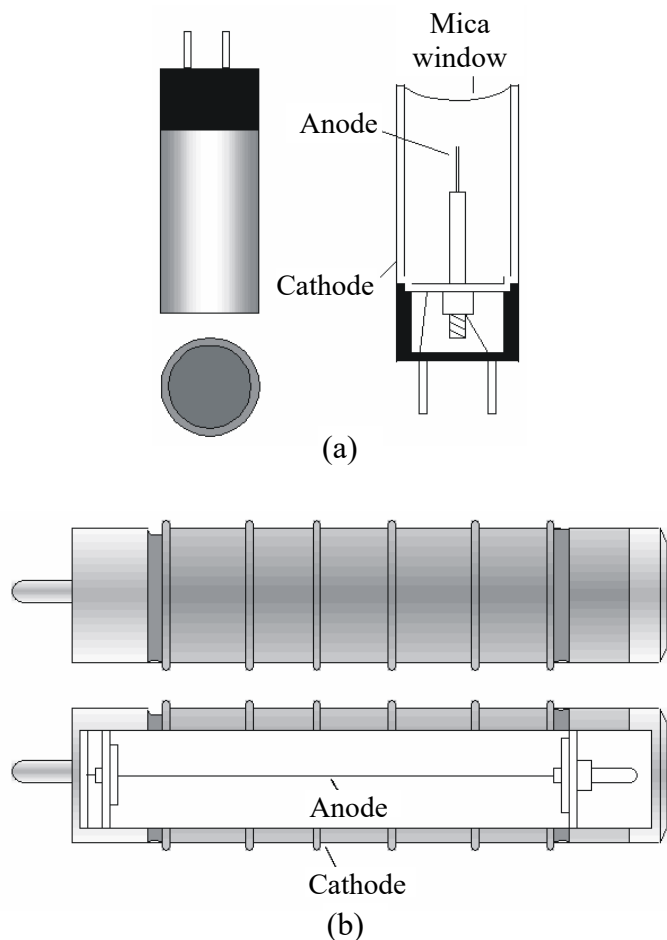


Fig. 8. Typical configurations of G-M tubes: (a) End-window type (radiation enters the tube through a thin mica window, which is at one end of the tube). (b) Windowless type (radiation enters the tube through its outer shell, including the cathode, so that particles with low penetration depth are filtered out).

can penetrate the end window. Mica is the preferred material of the entrance window because of its mechanical stability in micrometer-thin sheets (allowing it to withstand the mentioned pressure difference) and relative transparency to radiation with low penetration depth. The maximum efficiency of a Geiger counter with an end-window tube is achieved when the source of radiation is directly in front of the mentioned window.

2) **Windowless** G-M tubes do not have an entrance window for radiation (see Fig. 8b). Such G-M tubes are used for detecting more penetrating radiation, like gamma radiation, X-rays or beta particles with energy of the order of 100 keV or greater. These particles (especially gamma photons) penetrate the outer electrode (cathode) quite easily, so that there is no need to make a special entrance window for them. The maximum efficiency of a Geiger counter with a windowless G-M tube is achieved by maximizing the solid angle subtended by the G-M tube when viewed from the source of radiation. This means that the G-M tube should be perpendicular to the line connecting the center of the tube and the source of radiation. However, if the number of particles emitted by an isotropic point source per unit time is known, and one needs to calculate the number of particles that entered the detector during a given measurement, then it may be more convenient to place the source on the symmetry axis of the detector, because then the cross-sectional area of the detector when viewed from the source is a circle, which simplifies calculation of the corresponding solid angle.

4.7. Quenching of secondary Geiger discharges

After the primary Geiger discharge, positive ions drift slowly towards the cathode. When a positive ion is neutralized at the cathode (i.e., when the ion accepts an electron from the cathode material), a certain amount of energy is released. This energy is equal to the difference of the ionization energy of the gas molecule and the work function (A) of the cathode. If this difference is greater than A , then the released energy may cause immediate emission of an additional electron from the cathode. For example, if the gas is argon (with ionization energy of 15.7 eV) and $A = 4$ eV, then $15.7 - 4 = 11.7$ eV will be released. Since this value is greater than A , an additional electron may be emitted from the cathode. The emission of the additional electron may also be mediated a photon. I.e., the mentioned energy difference may be emitted in the form of a photon, which then ionizes a gas molecule or (more likely) is absorbed by the cathode, causing emission of a photoelectron. Thus, neutralization of positive ions at the cathode may cause emission of additional electrons, if the ionization energy of the gas molecule is at least twice greater than the cathode work function A . Although probability of such an event after neutralization of a *single* ion is always extremely low, it may become close to 1 if the number of ions is very large. Under these conditions, each Geiger discharge will almost certainly cause a secondary Geiger discharge, if electric field at the moment of neutralization of most ions is sufficiently strong for a Geiger discharge. Consequently, the counter will generate a continuous sequence of pulses even after removing external radiation.

Since each particle hitting a Geiger counter must cause only one Geiger discharge (i.e., one voltage pulse), secondary Geiger discharges must be eliminated (“quenched”). There are two methods to ensure that neutralization of positive ions at the cathode does not cause secondary Geiger discharges:

- 1) slowing down the growth of electric field strength so that no positive ions remain inside the counter at the moment of time when the electric field becomes sufficiently strong for a Geiger discharge,
- 2) modifying the composition of the gas so that the energy released during neutralization of positive ions at the cathode does not cause emission of electrons or photons, but is used up in a different process instead (for example, dissociation of gas molecules).

Accordingly, there are two methods of quenching: external quenching and internal quenching, which are described below.

External quenching is achieved by increasing the load resistance R (see Fig. 4) to values of the order of $(10^8 - 10^9) \Omega$, so that the time constant RC of the detector becomes much greater than the time of ion drift from the anode to the cathode (a few milliseconds or longer). In the case of external quenching, the time dependence of electric field strength is approximately proportional to $1 - \exp(-t / RC)$, where t is the time since creation of primary ion pairs. A drawback of such approach is that the “dead time” of the counter (i.e., the minimum time that must pass since detecting a particle in order for the counter to be able to detect another particle) is of the order of RC , i.e., relatively large.

Internal quenching (also called **self-quenching**) is implemented by adding a small amount (5 % to 10 %) of another gas (quenching gas”), which has the following properties:

- 1) ionization energy of molecules of the quenching gas is less than ionization energy of molecules of the main gas,
- 2) neutralization of positive ions of the quenching gas does not cause emission of electrons or photons,
- 3) the quenching gas absorbs ultraviolet radiation much stronger than the main gas, and this absorption is not accompanied by photoionization.

Since each ion of the main gas collides with a large number (of the order of 10^4) of neutral molecules on its way to the cathode, it will eventually collide with a molecule of the quenching gas. As it follows from the first property mentioned above, transition of an electron from a molecule of the quenching gas to a molecule of the main gas causes a decrease of the total internal energy of such system of two molecules (this decrease is equal to the difference of the two ionization energies). Consequently, the mentioned transition can happen spontaneously, if the two molecules are sufficiently close to each other. Thus, a positive ion of the main gas becomes a neutral molecule of the main gas, and a neutral molecule of the quenching gas becomes a positive ion of the quenching gas. As a result, the positive ions that reach the cathode are those of the quenching gas (not the main gas).

A spontaneous decrease of internal energy of any physical system means that the same amount of energy is released in some form or other. In the previous paragraph, the term “internal energy” was used to mean only the energy of the *electronic* subsystem of the molecule. A peculiarity of the quenching gas is that the energy released during the mentioned electron transfer between two molecules is not emitted in the form of a photon, but is used up for excitation of vibrations and rotation of the molecule of the quenching gas (i.e., a part of the electronic energy is converted into kinetic energy of the atoms composing the molecule). This peculiarity is also the reason of the second property mentioned above: the energy released during neutralization of a positive molecular ion of the quenching gas at the cathode is converted into kinetic energy of the atoms composing the molecule. However, the additional kinetic energy is in this case large enough to cause dissociation of the molecule. This means that neutralization of the positive molecular ion of the quenching gas is accompanied by breaking up the molecule into two or more parts (atoms or molecular fragments).

Because of the third property mentioned above, the quenching gas absorbs the majority of photons emitted due to excitation of molecules. This also reduces the probability of a secondary Geiger discharge (which, as mentioned, can be mediated by a photon).

The mentioned properties are common to various polyatomic gases, such as ethanol (C_2H_5OH), ethylene (C_2H_4), methane (CH_4), and diatomic gases of halogens (Cl_2 , Br_2 , I_2). Ionization energies of these molecules are less than ionization energy of noble gases (for example, ionization energies of ethanol and argon are equal to 11.7 eV and 15.7 eV, respectively). Organic molecules (for example, ethanol) do not recombine after dissociation, so that the operating time of a Geiger counter with organic quenching gas is limited to $10^9 - 10^{10}$ Geiger discharges. Halogenic quenching gases do not have this drawback: their molecules recombine after dissociation.

4.8. Counting curve of a Geiger counter

Geiger counters are very sensitive to ionizing radiation. However, they are unable to identify the type of the incident radiation or to measure energy of incident particles. They can be used only for particle counting. An ideal Geiger counter is the one that detects every particle, which causes ionization inside the G-M tube. This means that the counting device (a ratemeter), which accepts the voltage pulses from the G-M tube, must have the detection threshold smaller than the minimum pulse height generated by the G-M tube. If the voltage applied to the G-M tube is less than a certain value, then the Geiger discharge is impossible, so that the pulse height is practically zero. Consequently, the counting rate (the average number of counts per unit time) is also zero. Even when the Geiger discharge is possible, the heights of pulses generated by real G-M tubes are not identical, and some of them may be less than the detection threshold. If the voltage is increased, then the average pulse height and the fraction of pulses higher than the detection threshold increase, too. Consequently, the counting rate also increases with voltage. The dependence of the counting rate on the detector voltage is called the **counting curve** of the Geiger counter. Examples of counting curves are shown in Fig. 9. The starting voltage of a counting

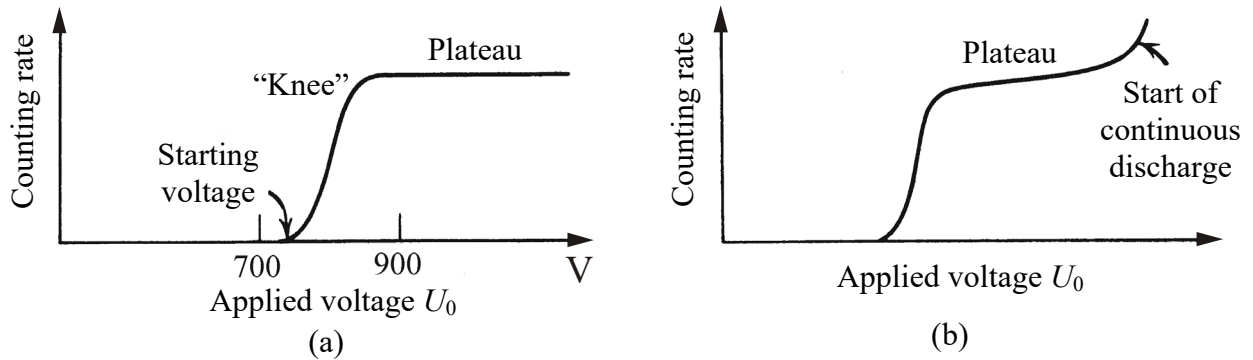


Fig. 9. Examples of a counting curve of a Geiger counter. (a) The ideal case, when the heights of all pulses generated by the G-M tube are greater than the detection threshold of the counting device connected to the tube, starting from a certain value of the tube voltage U_0 . In this case, the mentioned value of U_0 corresponds to the start of the plateau (in this example, it is approximately equal to 900 V), and the slope of the plateau is exactly zero. (b) The case of a realistic Geiger counter, where pulses with heights less than the detection threshold exist at all values of the applied voltage. The fraction of such pulses decreases with increasing voltage U_0 (that is to say, the fraction of detectable pulses increases with U_0), causing a positive slope of the plateau.

curve of a Geiger counter is usually between 300 V and 1000 V. The region of the counting curve with the smallest slope is called the **Geiger plateau**.

Thus, the non-zero slope of the Geiger plateau is mainly caused by existence of pulses with heights below the detection threshold, and dependence of the number of such pulses on the applied voltage. Pulses with amplitudes much less than the average value may occur due to various reasons. For example, if a primary ionization event occurs when the electric field strength has not yet reached its maximum value after the previous Geiger discharge, then the resulting pulse will have a reduced height. Another factor is inhomogeneous distribution of electric field strength along the anode: the field is weaker at the ends of the G-M tube than near its center. Consequently, Geiger discharges that begin at the ends of the G-M tube may be smaller than discharges that begin near the center of the G-M tube.

The Geiger plateau extends to a particular limiting value of the applied voltage. If this limiting voltage is exceeded, then a continuous discharge begins in the G-M tube. It may be either a corona discharge near the irregularities of the anode surface, or a continuous sequence of Geiger discharges due to failure of the quenching methods described in Section 4.7.

The Geiger plateau corresponds to the optimal range of applied voltage, in the sense that the counting rate is least affected by unforeseen variations of applied voltage (which cannot be absolutely stable). Consequently, the width and slope of the Geiger plateau are among the parameters that are used to evaluate quality of a Geiger counter: a wider Geiger plateau and a smaller value of its slope usually indicate higher quality of a counter. The width of the Geiger plateau of most Geiger counters is a few hundreds volts, values of its slope usually belong to the interval (0.01 – 0.1) % / V, and the optimal operating voltage is typically (300 – 500) V (for counters with halogen quenching) or around 1 kV (for other types of Geiger counters).

4.9. Dead time of a Geiger counter and a method of measuring it

4.9.1. The concept of the dead time and its underlying physics in the case of a Geiger counter

The **dead time** (τ_d) of a detector is the time that must pass after detecting a particle in order for the detector to be able to detect another particle. If the next particle interacts with the active medium of the detector before the time τ_d has passed, it will not be detected (i.e., the detector will not generate a voltage pulse, or the height of the pulse will be less than the detection threshold). Since the dead time of any real detector is non-zero, the counting rate is always reduced (i.e., always less than the rate of primary ionization events in the detector). Thus, a non-zero value of τ_d causes a systematic error of the counting rate.

The main reason of reduced sensitivity of a Geiger counter to ionizing radiation during the time τ_d after detecting a particle is the temporary reduction of electric field strength near the anode after a Geiger discharge (see Section 4.5). Since a Geiger discharge becomes possible only when the electric field strength exceeds a certain threshold value, a particle will not be detected if it hits the detector before the mentioned threshold is exceeded. Even after the electric field strength exceeds the mentioned threshold, it

will take some time to reach the maximum value. If a Geiger discharge occurs before the maximum electric field strength has been restored, then a reduced number of free electrons will be created, hence the output voltage pulse of the G-M tube will be reduced, too, and it may be less than the detection threshold of the external counting device (so that the pulse will not be counted).

Thus, the dead time of a Geiger counter is approximately equal to the time needed for the electric field strength near the anode to reach the value sufficient for registering a Geiger discharge. The rate of growth of electric field strength after a Geiger discharge is different for the counters with internal quenching and with external quenching (see Section 4.7). In the case of internal quenching, the dead time is determined by the time t_i needed for positive ions to recede to a sufficient distance from the anode. In the case of external quenching, the dead time is determined by the time constant RC of the counter system (see Fig. 4). This time constant is always much greater than t_i , because otherwise the external quenching would not be effective (see Section 4.7). For this reason, dead times of counters with external quenching are relatively large (typically $10^{-3} - 10^{-2}$ s) in comparison with dead times of counters with internal quenching (typically $5 \times 10^{-5} - 10^{-4}$ s). It should also be noted that the dead time of the entire counting system (G-M tube plus the external registering device, which counts the pulses generated by the G-M tube) may also be affected by the timing characteristics of the registering device connected to the G-M tube. If the “dead time” of the registering device is much greater than the dead time of the G-M tube, then the dead time of the registering device will determine the overall dead time of the counting system.

Even if a particle is not counted, it may cause some temporary changes that affect the ability of the detector to register the next particle. For example, in the case of a Geiger counter, any interaction of a particle with the detector, including those interactions that occur during the “dead time”, may cause a reduction of electric field strength (due to the processes described in Section 4.5), so that subsequent full restoration of electric field is postponed. Thus, the dead time may be extended. However, this effect becomes important only in the case of a relatively large probability that two or more particles will interact with the detector while it has not yet fully recovered from the previous interaction event. Such a situation is rarely encountered in practice. Hence it will be further assumed that no more than one particle may interact with the detector during the time τ_d since detection of the previous particle.

4.9.2. Measuring the dead time of a detector by the method of two sources

First, we will derive an expression of the counting rate N in terms of the dead time τ_d and the “true” counting rate N_0 (the frequency of *interaction* events, which would be measured in the ideal case $\tau_d = 0$). As it follows from the definition of the counting rate N , the average number of particles detected by the counter during the time $t \gg \tau_d$ is equal to Nt . Each detection of a particle was followed by a time interval of duration τ_d when the counter was insensitive to radiation. Consequently, the total time when the counter was insensitive to radiation is equal to $Nt\tau_d$. As it follows from the definition of N_0 , the true number of interaction events during the latter interval of time is equal to $N_0Nt\tau_d$, and the total number of interaction events during the time t is equal to N_0t . The latter number can also be expressed as the sum of the number of detected particles (i.e., number of interaction events that were counted by the detector) and the number of interaction events that were missed due to the dead time of the detector:

$$N_0t = N_0Nt\tau_d + Nt,$$

or

$$N_0 = \frac{N}{1 - N\tau_d}. \quad (4.9.1)$$

Thus, if the dead time τ_d is known, then the “true” counting rate N_0 can be obtained by correcting the measured counting rate N according to Eq. (4.9.1). From Eq. (4.9.1) the following expression of N is obtained:

$$N = \frac{N_0}{1 + N_0\tau_d}. \quad (4.9.2)$$

If $N_0 \rightarrow \infty$, then the right-hand side of Eq. (4.9.2) approaches $1 / \tau_d$, i.e., $N\tau_d$ approaches 1. Thus, the measured counting rate can never exceed the inverse dead time, i.e., $N\tau_d$ is always less than 1. Eqs. (4.9.1) and (4.9.2) are applicable only when $N\tau_d$ is *much* less than 1 (or less than about 0.2), because otherwise the probability of two or more particles interacting with the detector during its dead time may become sufficiently large, causing the dead time extension mentioned above (and consequently an even greater reduction of the measured counting rate).

Eq. (4.9.1) could be applied to measure τ_d as follows. The counting rate could be measured at two different distances between the source and the detector, producing two values of the measured counting rate (N_1 and N_2). If the ratio of the corresponding true counting rates (N_{01} and N_{02}) is known (it will be denoted f), then a system of two simple algebraic equations with two unknowns τ_d and N_{01} is obtained by writing Eq. (4.9.1) for each of the two measurements, i.e., by replacing N_0 with N_{01} or $N_{02} = fN_{01}$ on the left-hand side, and by replacing N with N_1 or N_2 on the right-hand side. However, it would be difficult to obtain the exact value of f beforehand. A modification of this method is based on the fact that the number of particles hitting the detector from *two* simultaneous sources of radiation is *exactly* equal to the sum of the numbers of particles reaching the detector from each source separately (assuming that neither one of those sources significantly scatters the radiation of another one). The true counting rates corresponding to each of the two sources will be denoted N_{01} and N_{02} . Three measurements of the counting rate would have to be performed: counting rate of source No. 1 (N_1), counting rate of source No. 2 (N_2), and simultaneous counting rate of both sources (N_{12}). Then a system of three algebraic equations with three unknowns τ_d , N_{01} and N_{02} is obtained by writing Eq. (4.9.1) for each of the three measurements, i.e., by replacing N_0 with N_{01} , N_{02} or $N_{01} + N_{02}$ on the left-hand side, and by replacing N with N_1 , N_2 or N_{12} on the right-hand side. Yet another minor modification is related to the fact that the true counting rate usually includes a small constant term reflecting the constant radiation “background” (for example, natural radiation of the environment). In order to take into account the background radiation, it has to be measured separately (with both sources removed). The corresponding measured counting rate will be denoted N_b , and the corresponding true counting rate will be denoted N_{0b} . Thus, four equations are obtained:

$$N_{0b} = \frac{N_b}{1 - N_b \tau_d}, \quad N_{0b} + N_{01} = \frac{N_1}{1 - N_1 \tau_d}, \quad N_{0b} + N_{02} = \frac{N_2}{1 - N_2 \tau_d}, \quad N_{0b} + N_{01} + N_{02} = \frac{N_{12}}{1 - N_{12} \tau_d}. \quad (4.9.3)$$

Since the number of equations is equal to the number of unknowns (τ_d , N_{0b} , N_{01} , and N_{02}), this system of four equations has a unique solution. It is replaced by a single equation with respect to τ_d by observing that the left-hand side of the fourth equation can be obtained by adding up the left-hand sides of the second and third equations, and subtracting the left-hand side of the first equation:

$$\frac{N_1}{1 - N_1 \tau_d} + \frac{N_2}{1 - N_2 \tau_d} - \frac{N_b}{1 - N_b \tau_d} = \frac{N_{12}}{1 - N_{12} \tau_d}. \quad (4.9.4)$$

After multiplying by the common denominator, the latter equation can be written as a fourth-degree polynomial equation with respect to the dead time τ_d . Its solution is

$$\tau_d = \frac{X(1 - \sqrt{1 - Z})}{Y}, \quad (4.9.5a)$$

where

$$X = N_1 N_2 - N_b N_{12}, \quad (4.9.5b)$$

$$Y = N_1 N_2 (N_{12} + N_b) - N_b N_{12} (N_1 + N_2), \quad (4.9.5c)$$

$$Z = \frac{Y(N_1 + N_2 - N_{12} - N_b)}{X^2}. \quad (4.9.5d)$$

The uncertainty of the value of τ_d calculated according to Eqs. (4.9.5a–d) depends on uncertainties of the measured values of N_b , N_1 , N_2 and N_{12} . In order to simplify combining the mentioned four uncertainties, an approximate solution of Eq. (4.9.4) may be used. This simplification relies on the assumption

$$N_b \tau_d \ll 1, \quad N_1 \tau_d \ll 1, \quad N_2 \tau_d \ll 1, \quad \text{and} \quad N_{12} \tau_d \ll 1 \quad (4.9.6)$$

(those inequalities are usually satisfied in practice). By applying the approximate mathematical identity $1/(1-x) \approx 1+x$ (which is applicable when $x \ll 1$), Eq. (4.9.4) is replaced by the following linear equation:

$$N_1(1 + N_1 \tau_d) + N_2(1 + N_2 \tau_d) - N_b(1 + N_b \tau_d) \approx N_{12}(1 + N_{12} \tau_d). \quad (4.9.7)$$

Its solution is

$$\tau_d \approx \frac{N_1 + N_2 - N_b - N_{12}}{N_{12}^2 - N_1^2 - N_2^2 + N_b^2}. \quad (4.9.8)$$

The general rule of combining uncertainties of several variables (x_1, x_2, \dots, x_n) when calculating the uncertainty of another quantity y , which is a function of the mentioned variables, is the following:

$$\Delta y = \sqrt{\left(\frac{\partial y}{\partial x_1}\right)^2 (\Delta x_1)^2 + \left(\frac{\partial y}{\partial x_2}\right)^2 (\Delta x_2)^2 + \dots + \left(\frac{\partial y}{\partial x_n}\right)^2 (\Delta x_n)^2}, \quad (4.9.9)$$

where Δy is the uncertainty of y , and $\Delta x_1, \Delta x_2, \dots, \Delta x_n$ are the uncertainties of x_1, x_2, \dots, x_n . In the case discussed, “ y ” is the dead time τ_d , and the arguments “ x_i ” ($i = 1, 2, 3, 4$) have the meaning of N_b, N_1, N_2 , and N_{12} . In order to further simplify calculation of the partial derivatives in Eq. (4.9.9), the denominator of Eq. (4.9.8) may be assumed to be approximately constant (this assumption is also justified by the conditions (4.9.6)). In this way, the following approximate expression of the uncertainty of τ_d is obtained from Eqs. (4.9.8) and (4.9.9):

$$\Delta \tau_d \approx \frac{\sqrt{(\Delta N_1)^2 + (\Delta N_2)^2 + (\Delta N_b)^2 + (\Delta N_{12})^2}}{N_{12}^2 - N_1^2 - N_2^2 + N_b^2}, \quad (4.9.10)$$

where $\Delta N_b, \Delta N_1, \Delta N_2$ and ΔN_{12} are the uncertainties of N_b, N_1, N_2 , and N_{12} .

Since this method of determining the dead time τ_d relies on measuring the difference of two very similar numbers (N_{12} and $N_1 + N_2 - N_b$), it is important to ensure high accuracy of the measurements. This means that the position of each source relative to the detector when N_{12} is measured (i.e., when both sources are used simultaneously) must be exactly the same as in the case when N_1 or N_2 is measured (i.e., when only one source is used). In order to satisfy this requirement, the optimal sequence of measurements is the following: after measuring N_1 , the second source is placed near the detector (taking care to not touch the first source or the detector), then N_{12} is measured, then the first source is removed (taking care to not touch the second source or the detector), and N_2 is measured.

4.10. Efficiency of a Geiger counter

4.10.1. The concepts of absolute or relative efficiency of a detector

A detector generates a voltage pulse only when the incident particle interacts with the active medium of the detector (i.e., ionizes an atom of the active medium). If the incident particle is charged (for example, alpha and beta particles), then probability of interaction per unit path is large, hence the particle begins to interact with the active medium immediately after entering the detector (this interaction is electrostatic, i.e., the incident particle interacts with electrons and atomic nuclei of the active medium by the Coulomb force). Consequently, it is relatively easy to ensure that every alpha or beta particle that has entered the active medium of the detector is detected (i.e., causes a voltage pulse at the output of the sensing element, such as a G-M tube). However, the mean path of a neutral particle (for example, gamma photon or neutron) until an interaction event is much longer than the mean free path of a charged particle. Consequently, it is possible that a neutral particle will not be detected even after entering the active medium of the detector (because the particle did not collide with any atom of the active medium).

In order to characterize the ability of a detector to detect various particles, the concept of detector efficiency is used. Detector efficiency can be defined in two ways:

- 1) **absolute efficiency** ε_{abs} is the ratio of the number of detected particles to the number of particles emitted by the radioactive source,
- 2) **intrinsic efficiency** ε is the ratio of the number of detected particles to the number of particles that have entered the sensing element of the detector (such as a G-M tube).

The absolute efficiency depends not only on properties of the detector and of the incident radiation, but also on the geometry of the measurements (especially on the distance between the source and the detector), because the relative geometrical arrangement of the detector and the source determines the fraction of emitted particles that hit the detector. The intrinsic efficiency does not depend on the relative positions of the source and the detector. It is therefore more suitable to characterize sensitivity of a detector to incident radiation of a particular type (unless the detector is designed to operate with sources placed in a strictly defined position, so that the fraction of particles hitting the sensing element is also fixed). In the case of an isotropic point source (which emits particles in all direction equally), the absolute and intrinsic efficiencies are related to each other as follows:

$$\varepsilon = \varepsilon_{\text{abs}} \frac{4\pi}{\Omega}, \quad (4.10.1)$$

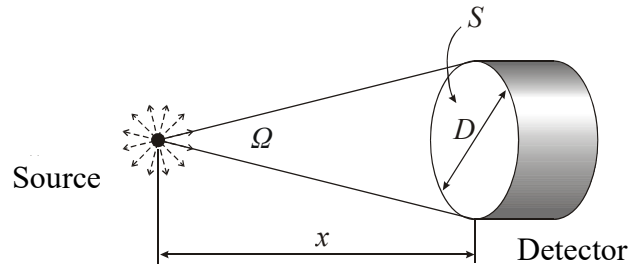


Fig. 10. A typical measurement geometry

where Ω is the solid angle subtended by the active region of the detector from the point of the source. Intrinsic efficiency will be further referred to simply as “efficiency”.

The source of radiation is frequently small enough to be approximated by a point source. In the case of the measurement geometry shown in Fig. 10, the solid angle is equal to

$$\Omega = 2\pi \left[1 - \frac{x}{\sqrt{x^2 + (D/2)^2}} \right], \quad (4.10.2)$$

where x is the distance between the source and the detector, and D is the diameter of the front surface of the detector (or of the entrance window that is on the front surface of the detector). If $x \gg D$, then the solid angle is approximately equal to the ratio of the area S of the front surface of the detector and the distance x squared:

$$\Omega \approx \frac{S}{x^2} = \frac{\pi D^2}{4x^2}, \quad (4.10.3)$$

i.e., the solid angle (and the number of detected particles) is inversely proportional to the distance squared. The relative error of the approximate expression (4.10.3) in comparison with the exact expression (4.10.2) decreases rapidly with increasing x . For example, when $x = 3D$, the mentioned relative error is only 2 %.

4.10.2. Underlying physics, typical values, and methods of increasing efficiency of a Geiger counter

Charged particles (for example, alpha and beta particles), which have entered the active volume of a gaseous radiation detector of a typical size ((2 – 10) cm), usually create at least one primary ion pair (a free electron and a positive ion). In the case of a Geiger counter, even a single free electron initiates a Geiger discharge, causing a voltage pulse of a sufficiently large height at the output of the G-M tube. Consequently, efficiency of Geiger counter for charged particles is close to 100 %. Under these conditions, the only factor that may reduce the efficiency of the counter is absorption or backscattering of the incident charged particles in the entrance window of the G-M tube. In order to reduce these particle losses, the mass thickness of the entrance window (i.e., the product of its density and thickness) must be sufficiently small, typically (3 – 10) mg/cm². In the case of mica (the preferred material of the entrance window), those values of the mass thickness correspond to thickness of approximately 10 μm.

Probability of interaction of a gamma photon with matter is much less than that of an alpha or beta particle. Consequently, efficiency of gaseous detectors when detecting gamma radiation is typically only (2 – 4) %. If the energy of gamma photons is greater than 100 keV, then they almost do not interact with the fill gas of the G-M tube. Instead, gamma photons of such energies interact almost exclusively with the outer shell of the G-M tube (including the cathode). A result of interaction of a gamma photon with an atom is emission of an electron from the atom. Consequently, almost all primary ion pairs in the fill gas are created by electrons emitted from the cathode by the incident gamma radiation. Thus, efficiency of a Geiger counter used for detecting gamma radiation is determined by two factors:

- 1) probability that a gamma photon will interact with the material of the cathode of the G-M tube, causing emission of an electron from an atom of the material,
- 2) probability that the mentioned free electron will reach the fill gas, i.e., that it will exit the cathode through its inner surface (rather than being stopped inside the material of the cathode or exiting through its outer surface).

All electrons, which can reach the fill gas of a G-M tube, are emitted in a thin inner layer of the cathode (see Fig. 11). A typical range (i.e., maximum path before being stopped) of an electron with initial energy

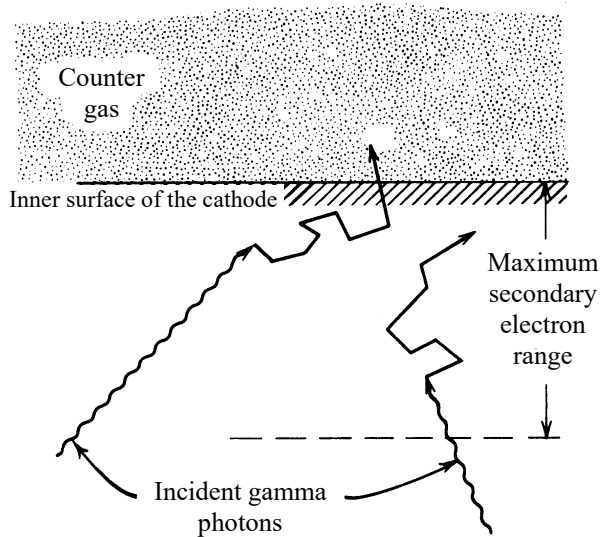


Fig. 11. The main process responsible for sensitivity of G-M tubes to gamma radiation is emission of secondary electrons inside the cathode. Only the electrons emitted at a distance less than their range from the inner surface of the cathode can initiate a Geiger discharge.

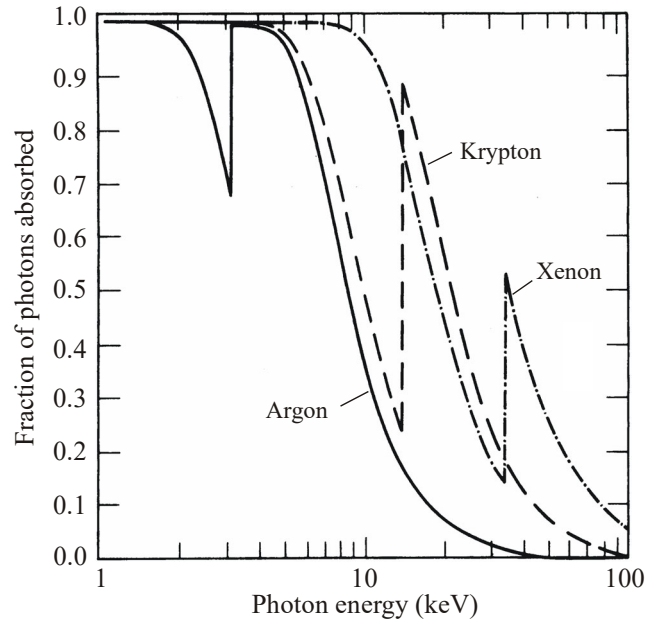


Fig. 12. Energy dependence of the fraction of photons absorbed in a 5.08 cm thick layer of various gases at standard atmospheric pressure (about 10^5 Pa)

of a few hundred keV inside the material of the cathode is (1 – 2) mm. If the cathode thickness is greater than that, then the probability of interaction of the incident gamma photon with the material of the cathode will increase, but efficiency of the Geiger counter will not increase, because electrons that were emitted at a greater depth will not be able to reach the inner surface of the cathode.

In order to increase probability of interaction of a gamma photon with the mentioned sensitive layer of the cathode, the atomic number (Z) of the material of the cathode must be sufficiently large. For example, G-M tubes with bismuth (Bi) cathode were extensively used in the past for detecting gamma radiation (the atomic number of bismuth is $Z = 83$).

If the energy of gamma photons is sufficiently small (~ 10 keV or less), then probability of their interaction with the fill gas of the G-M tube may become sufficient to achieve efficiency of the order of 10 %, or even close to 100 %. Sensitivity of a Geiger counter to low-energy gamma or X-ray radiation can be improved using a fill gas with a sufficiently large atomic number and at a sufficiently high pressure. The fill gas of G-M tubes designed to detect gamma or X-ray radiation is usually xenon (Xe) or krypton (Kr). Efficiency of Geiger counters with such G-M tubes can be as high as 100 % when the photon energy is less than 10 keV (see Fig. 12).

5. Experimental setup and measurement procedure

5.1. Experimental equipment

The Geiger counter that is used for this experiment consists of an end-window G-M tube (of the type shown in Fig. 8a) and a ratemeter manufactured by **Isotrak**. The equipment is shown in Fig. 13.

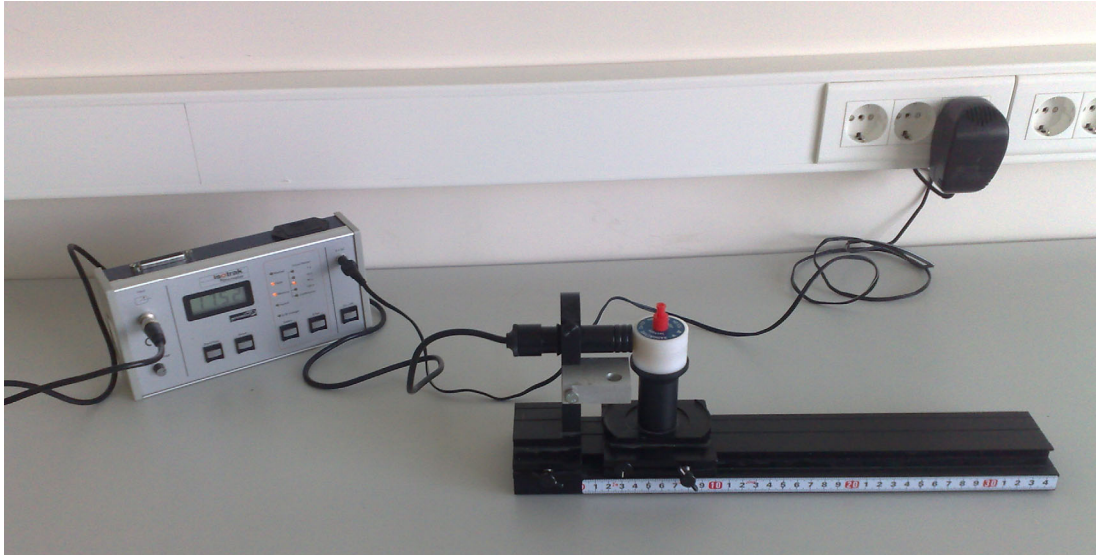


Fig. 13. The experimental equipment. The ratemeter is on the left, the G-M tube is in the center, the gamma source is placed on a holder in front of the G-M tube. The source holder may be moved along the optical bench, thus changing the distance between the source and the G-M tube.

Technical data of the G-M tube:

Mass thickness of the entrance window: 1.5 – 2.0 mg/cm²

Material of the entrance window: Mica

Effective diameter of the window: $D = 9 \text{ mm}$

Fill gas: neon / argon, with halogen quenching

Two identical sources of gamma radiation are used for this experiment. **The activity of each source was last measured in 2001. Then it was equal to 370 kBq = 3.7×10^5 decays / s. The decay half-life of ¹³⁷Cs is equal to 30,04 years.**

In each source, the radioactive material is a mixture of beta-radioactive ¹³⁷Cs and gamma-radioactive isotope of barium ^{137m}Ba, which is a product of beta decay of ¹³⁷Cs. Beta particles (electrons) emitted during the beta decay of ¹³⁷Cs are completely absorbed by the plastic walls of the source enclosure, so that only gamma photons emitted by ^{137m}Ba escape into the environment. The letter “m” in the subscript “137m” indicates a long-lived (“metastable”) excited energy level of ¹³⁷Ba. Each gamma photon is created during the quantum transition of a ¹³⁷Ba nucleus from this excited state to the lowest-energy state (the “ground state”).

5.2. Measurement procedure

1. Switch on the **Isotrak** ratemeter. Reduce the G-M tube voltage to the lowest value achievable by turning counter-clockwise the knob, which is in the lower left corner of the control panel (see also the **Isotrak** user manual in Section 5.3).
2. Place one of the two ¹³⁷Cs sources on the holder in front of the G-M tube, as shown in Fig. 13. Gradually increase the applied voltage until the counting begins. The simplest method to determine if the Geiger counter is able to detect particles while the applied voltage is shown on the display is based on the use of audible indication of pulses. The starting voltage is the smallest voltage when the beeps are heard (each beep corresponds to one voltage pulse at the output of the G-M tube). **Note:** The audible indication of pulses may be switched on or off as described in Section 5.3.
3. Increase the voltage to a value greater than the starting voltage by (10 – 20) V. This is the voltage of the first measurement. At this point, it is recommended to switch off the audible indication of pulses (see Section 5.3) in order to reduce the level of noise at the workplace.

4. Starting from the voltage value determined in Step 3, increase the voltage to approximately 600 V in steps of 20 V. At each value of the applied voltage, perform one count with duration of 1 min. Record the measurement data in a table with two columns: voltage in column 1, and number of detected gamma photons in column 2. Since the display of the ratemeter can show either the voltage or the number of detected particles, but not both simultaneously, the operating mode of the ratemeter must alternate between “G-M VOLTAGE” and “GATE” (see Section 5.3 for instructions on how to change the operating mode of the ratemeter).
5. Set the operating voltage to (500 ± 10) V (all remaining measurements will be performed at a fixed voltage). **(a)** Measure the background radiation. In order to do so, place the radioactive sources sufficiently far from the detector, so that they do not affect the counts (a distance of 2 m is sufficiently large). Care should be taken to not interfere with other radioactivity experiments that are being performed nearby at the same time. Perform 5 counts with duration of 1 min each. **(b)** Place one source (further called “source No. 1”) in the same position as before (i.e., on the holder in front of the detector, as shown in Fig. 13) and again perform 5 counts with duration of 1 min each. **(c)** Taking care to not touch source No. 1 or the G-M tube, place another source (“No. 2”) on the aluminum holder at the side of the G-M tube, as shown in Fig. 14. Again perform 5 counts with duration of 1 min each. **(d)** Taking care to not touch source No. 2, remove source No. 1 and place it sufficiently far from the detector. Again perform 5 counts with duration of 1 min each.
6. Place any one of the two sources in front of the detector (the other source must be sufficiently far from the detector). Increase the distance between the source and the detector from 5 cm to 25 cm in increments of 2.5 cm, performing one minute-long count at each distance. *Note:* The mentioned distance is the distance from the center of the source to the center of G-M tube. It is shown by the white mark at the bottom of the source holder (for example, in Fig. 15, the distance is 10 cm).
7. After finishing all measurements, switch off the ratemeter and show the tables with the measurement data to the laboratory supervisor for signing.

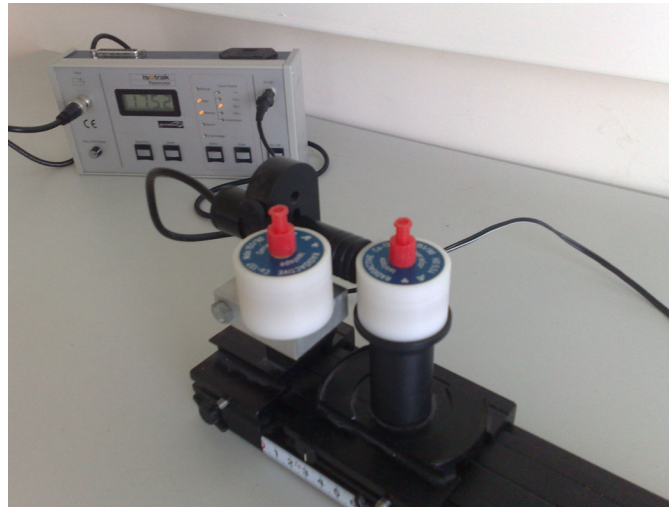


Fig. 14. Placement of the sources while measuring the dead time of the counter by the method of two sources

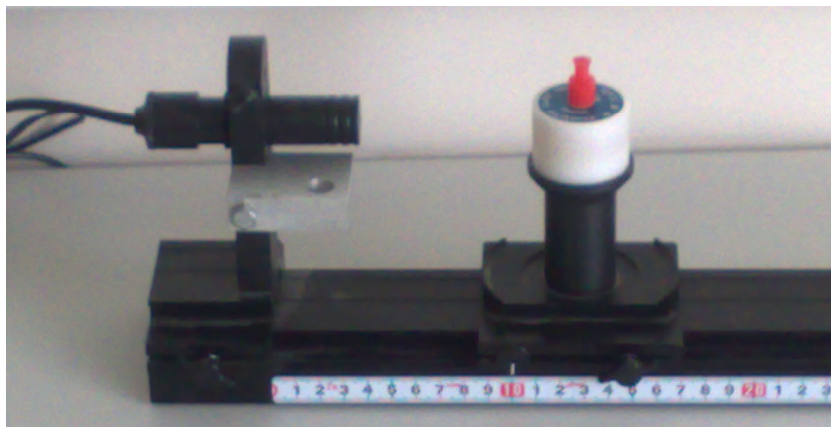


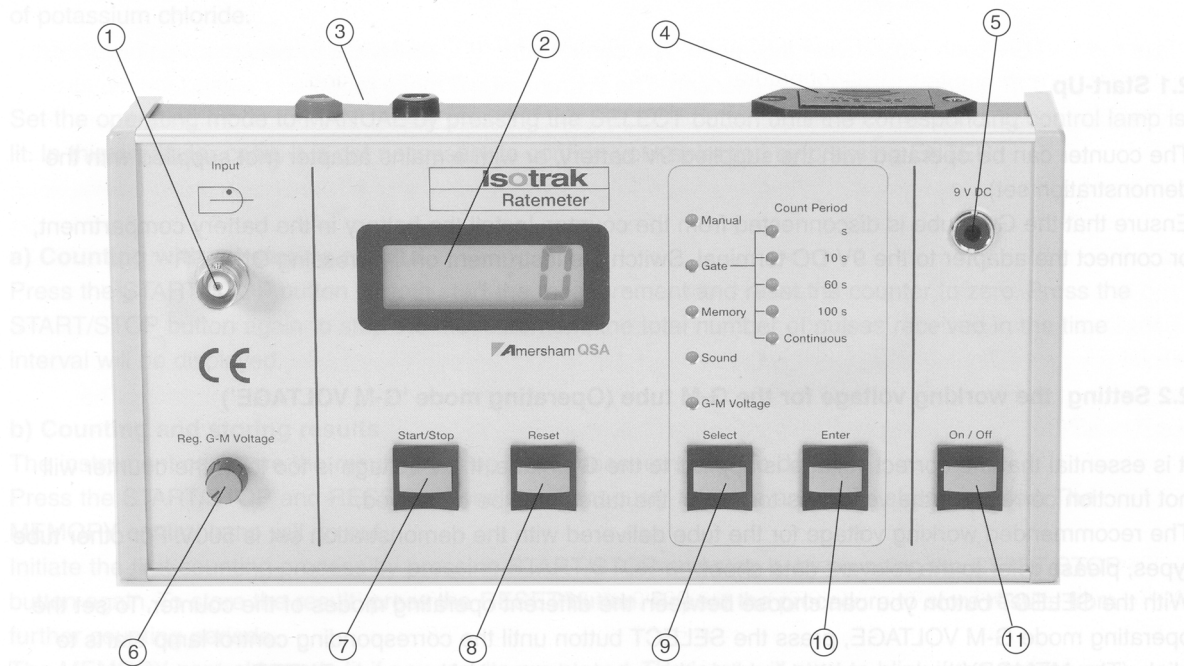
Fig. 15. Position of the radioactive source while measuring the dependence of the counting rate on the distance

5.3. Instruction manual of the Isotrak ratemeter

Below are four pages scanned from an Isotrak booklet that is included with the measurement equipment used for this experiment. The Geiger counter consists of a sensing element (the Geiger-Müller tube) and a ratemeter. The ratemeter has a built-in adjustable power supply for the detector, an LCD display for showing the counts, and buttons for selection of various counting modes. **Note:** This is supplementary information. The description of experimental setup and measurement procedure is in Sections 5.1 and 5.2.

1. Front panel of G-M counter

Caution! Before connecting the tube to the G-M counter make sure that the tube voltage has been set correctly (see also section 2.2).



Front panel of isotrak Ratemeter

- (1) INPUT terminal for the G-M tube
- (2) Display
- (3) TTL compatible interface
- (4) Compartment for 9V battery
- (5) 9V DC terminal for mains adapter
- (6) G-M tube voltage control
- (7) START/STOP button to start/stop the counting process
- (8) RESET button to clear the display only.
When the RESET and START/STOP buttons are pressed simultaneously, the memory will also be cleared.
- (9) SELECT button to choose operating modes and options
- (10) ENTER button to enter and leave operating modes
- (11) ON/OFF button

Control lamps: The selected operating mode is indicated by a lamp. The MEMORY lamp is lit when data have been stored, and starts blinking to indicate a memory overflow. During the measurement, the GATE lamp blinks rapidly to indicate that the counter is operating.

2. Operating modes of the G-M counter

This chapter describes how to operate the G-M counter and learn its operating modes by carrying out simple experiments. The experiments described in sections 2.4 to 2.6 are also suitable for introducing the subject of radioactivity to students.

2.1 Start-Up

The counter can be operated with the supplied 9V battery, or with a mains adapter (not supplied with the demonstration set).

Ensure that the G-M tube is disconnected from the counter. Install the battery in the battery compartment, or connect the adapter to the 9V DC terminal. Switch the instrument on by pressing ON/OFF.

2.2 Setting the working voltage for the G-M tube (Operating mode 'G-M VOLTAGE')

It is essential that the correct voltage is applied to the G-M tube. If the voltage is too low, the counter will not function correctly, if the voltage is too high, the tube could be destroyed.

The recommended working voltage for the tube delivered with the demonstration set is 500V. For other tube types, please refer to the relevant data sheet.

With the SELECT button you can choose between the different operating modes of the counter. To set the operating mode G-M VOLTAGE, press the SELECT button until the corresponding control lamp starts to blink. (The MEMORY lamp may start to blink; this can be ignored.) Now press ENTER to activate the currently selected operating mode. When the G-M VOLTAGE control lamp is lit, the tube voltage is indicated in the display. The only thing you have to do now is to set the voltage to the recommended voltage for your G-M tube by turning the REG. G-M VOLTAGE control. A small difference (a few volts) between the set voltage and the recommended voltage doesn't matter. If you want to leave the operating mode, press ENTER or simply switch off the instrument.

2.3 Audible indication of pulses (Operating mode 'SOUND')

Connect the lead from the G-M tube to the INPUT terminal. Leave the plastic cap over the fragile window of the G-M tube to prevent damage.

Press SELECT until the control lamp SOUND starts blinking and confirm by pressing ENTER. With SELECT you can now start or stop the audible indication of pulses (the display shows ON or OFF, respectively). With the G-M tube connected, you should now be able to hear the pulses caused by background radiation as short beeps. If you want to stop this operating mode, press ENTER or simply switch off the instrument.

2.4 Counting pulses (Operating mode 'MANUAL')

This section describes different methods to count the number of pulses measured in given time periods. For effective demonstrations, the pulse rate should be higher than the rate from background radiation. An increase in the pulse rate can be achieved by measuring the gamma radiation from the radioactive isotope K-40. All natural potassium compounds contain 0.01% K-40. Just insert the G-M tube into the supplied flask of potassium chloride.

Set the operating mode to MANUAL by pressing the SELECT button until the corresponding control lamp is lit. In this particular case, it is not necessary to confirm your selection by pressing ENTER.

a) Counting without storing results

Press the START/STOP button to both start the measurement and reset the counter to zero. Press the START/STOP button again to stop the measurement; the total number of pulses received in the time interval will be displayed.

b) Counting and storing results

The instrument can store the results from up to 50 measurements. To do this:

Press the START/STOP and RESET buttons simultaneously to erase any data already stored. The MEMORY control lamp will go out.

Initiate the first counting process by pressing START/STOP and stop it by pressing the START/STOP button again. To store the result, press the RESET button. Repeat the procedure to store results from further counting periods.

The MEMORY control lamp is lit if any results are stored. The lamp will start to blink if the maximum number of results (50) is exceeded (storage overflow).

2.5 Reading stored results (Operating mode 'MEMORY')

Press the SELECT button repeatedly until the MEMORY control lamp starts blinking (even if storage overflow has already been indicated!). The display will show the last value stored. Previous data points can be recalled by pressing ENTER. The stored data points can therefore be retrieved in reverse order; at the end of the list the display shows three dashes.

If required, the stored data can be called off a second time by repeating these steps.

2.6 Counting pulses for predefined periods (Operating mode 'GATE')

Press the SELECT button until the GATE control lamp starts blinking and press ENTER to confirm the selection. Press SELECT again to step through the available count times and press ENTER when the required time is indicated by a control lamp. The control lamp marked CONTINUOUS will start blinking. The instrument can now be either set to count for one time period, or set to run automatically.

a) One time period

Press SELECT and then START/STOP to start data collection; the instrument will count the number of pulses registered in the chosen count time. Press RESET to store the result in the memory.

b) Automatic counting (Operating mode 'CONTINUOUS')

In this mode, the instrument will store the results from repeated, consecutive, measurements.

Press the ENTER button to activate this mode. The control lamp (CONTINUOUS) will stop blinking. Press the START/STOP button to commence counting. The instrument will make repeated measurements, each for the selected time period. To stop the sequence, press the START/STOP button again.

At the end of each count period, the display pauses for about 5 seconds to show the number of pulses received, so that the result can be written down if needed. There is no delay between the counting periods, but pulses registered during the first 5 seconds of a count period are not shown; the display is instead used to show the result from the previous period.

There is an easier method to record the results, rather than writing them down between measurements: the results are also automatically stored in the memory. Up to 50 points can be stored if the memory has been cleared by pressing START/STOP and RESET simultaneously before starting the measurements. The results can then be retrieved following the method given in section 2.5.

6. Analysis of measurement data

1. Plot the measured counting curve. Locate the plateau in it (see Fig. 9b). Using the method of linear fitting (i.e., fitting by the linear function $n = A + B \cdot U_0$), determine the slope coefficient B of the plateau, and its uncertainty ΔB . The fitting line must be shown in the same graph as the counting curve. The linear fitting can be performed using various data analysis software, or using the formulas presented in Section 7. Only the points that belong to the plateau must be used for the linear fitting. The slope coefficient B is equal to the increase of the counting rate when the applied voltage is increased by 1 V, while all other measurement conditions are unchanged. This slope coefficient should be redefined so that it does not depend on the relative positions of the G-M tube and the radioactive source, and only depends on intrinsic properties of the G-M tube. With this aim in mind, the value of B must be divided by the average counting rate in the region of the plateau. The quantity obtained in this way is the *relative* increase of the counting rate when the applied voltage is increased by 1 V. This slope coefficient must be expressed in units of %/V. **Note:** The region of continuous discharge, which is shown in Fig. 9b, cannot be seen in this experiment (because the measurement equipment cannot generate the sufficiently high voltage needed for the continuous discharge). Thus, only the lower bound on the width of the plateau can be determined in this experiment (the true width of the plateau is greater). This also means that the mentioned linear fitting can be performed using all data points that are outside the initial region of fast growth of the counting rate while the voltage is still close to the starting voltage.

When determining the starting point of the plateau, one should keep in mind that large variations of the measured counting rate may be purely random (i.e., unrelated to changes of applied voltage). This is because the radioactive decay (which causes emission of gamma photons in this experiment) is a random process described by Poisson statistics. If all measurements are performed at identical conditions, then the *statistical average* of the measurement result is a constant, but *individual* counts may be significantly different from each other. If the average count N (i.e., average number of photons detected per 1 min) is of the order of 100 or greater, then, as it follows from properties of the Poisson distribution, approximately 68 % of all counts will deviate from N no more than by \sqrt{N} (i.e., will belong to the interval $[N - \sqrt{N}, N + \sqrt{N}]$), approximately 95 % of all counts will deviate from N no more than by $2\sqrt{N}$, and approximately 99.7 % of all counts will deviate from N no more than by $3\sqrt{N}$. For example, if the average number of photons detected in 1 min is 2000, then, after performing a sufficiently large number of 1-minute long measurements, on the average, 1 count in 20 would be greater than $2000 + 2\sqrt{2000} = 2089$ or less than $2000 - 2\sqrt{2000} = 1911$. Consequently, if the first available data point is 1950 and the remaining 10 or 20 data points are between 2000 and 2050, then one should still assume that the first point belongs to the plateau (rather than to the initial region of fast growth with U_0), and the first point should *not* be excluded from the linear fitting mentioned above.

2. Calculate the average counting rates N_b , N_1 , N_2 and N_{12} , which are used in the dead time calculation formulas (4.9.5a–d). Calculate the dead time τ_d . **Note:** The units of the calculated value of τ_d depend on the units of time used in the definition of the counting rate.

Calculate the uncertainties of the counting rates ΔN_b , ΔN_1 , ΔN_2 and ΔN_{12} , assuming that the results of individual counts are distributed according to the Poisson distribution. This means that the uncertainty (or, more precisely, standard deviation) of the average count (counting rate) N_1 is equal to $\sqrt{N_1}/t$, where t is the total duration of counting the particles, whose number is used to calculate the average N_1 . If the measurements were performed as described in Step 5 of the measurement procedure (see Section 5.2), then $t = 5$ min. The other three mentioned uncertainties must be calculated in the same way. Then calculate the uncertainty of the dead time ($\Delta \tau_d$) according to Eq. (4.9.10).

3. Calculate the flux I of gamma photons, i.e., the number of gamma photons emitted in all directions by the source per 1 s. This calculation requires knowledge of the current activity of the source (**activity** is the number of nuclei that disintegrate spontaneously per unit time during the process called “radioactive decay”). The current activity Φ of the source must be calculated from the main law of

radioactive decay, which states that activity of a radioactive substance decreases with time exponentially (assuming that the substance is not replenished or lost in any other way): $\Phi = \Phi_0 \cdot 2^{-\Delta t/T}$, where Φ_0 is the initial activity, Δt is the time that passed since measuring the initial activity, and T is the decay half-life. In order to obtain the number of photons emitted per unit time, it is necessary to take into account that not all nuclei decay by emitting a photon. As it is evident from the decay diagram of ^{137}Cs (see Fig. 16), only 94.6 % of nuclei of ^{137}Cs decay to the second excited energy level of ^{137}Ba (this is the metastable excited state $^{137\text{m}}\text{Ba}$ responsible for the gamma photons that are counted in this experiment). In addition, only 90 % of these excited nuclei of ^{137}Ba decay to the ground state by emitting a gamma photon (the remaining ones decay by internal conversion, i.e., by transferring the excitation energy directly to an electron orbiting the same nucleus). Consequently, in order to obtain the photon flux, the activity of ^{137}Cs must be multiplied by a factor equal to $0.946 \times 0.9 \approx 0.85$ (i.e., the decay of only 85 % of nuclei of ^{137}Cs is accompanied by emission of a photon). Thus, $I \approx 0.85 \Phi_0$.

4. Plot the dependence of the difference $N - N_b$, where N is the counting rate measured in Step 6 of the measurement procedure (see Section 5.2) and N_b is the background counting rate measured in Step 5a of the measurement procedure, on the inverse squared distance between the source and the G-M tube ($1/r^2$). According to Eqs. (4.10.1) and (4.10.3), this dependence should be approximately linear:

$$N - N_b = \frac{C}{r^2}, \quad (6.1)$$

where C is the slope coefficient, which is equal to $C = \varepsilon D^2 I / 16$. The slope C is calculated by the method of linear fitting, which is described in Section 7 (see also the beginning of the current section). Then calculate the efficiency:

$$\varepsilon = \frac{16C}{ID^2}. \quad (6.2)$$

Note: The meaning of quantities N , N_b and I is the number of gamma photons *per unit time*. This unit of time must be the same everywhere (because the units of time must cancel out when calculating the right-hand side of Eq. (6.2)).

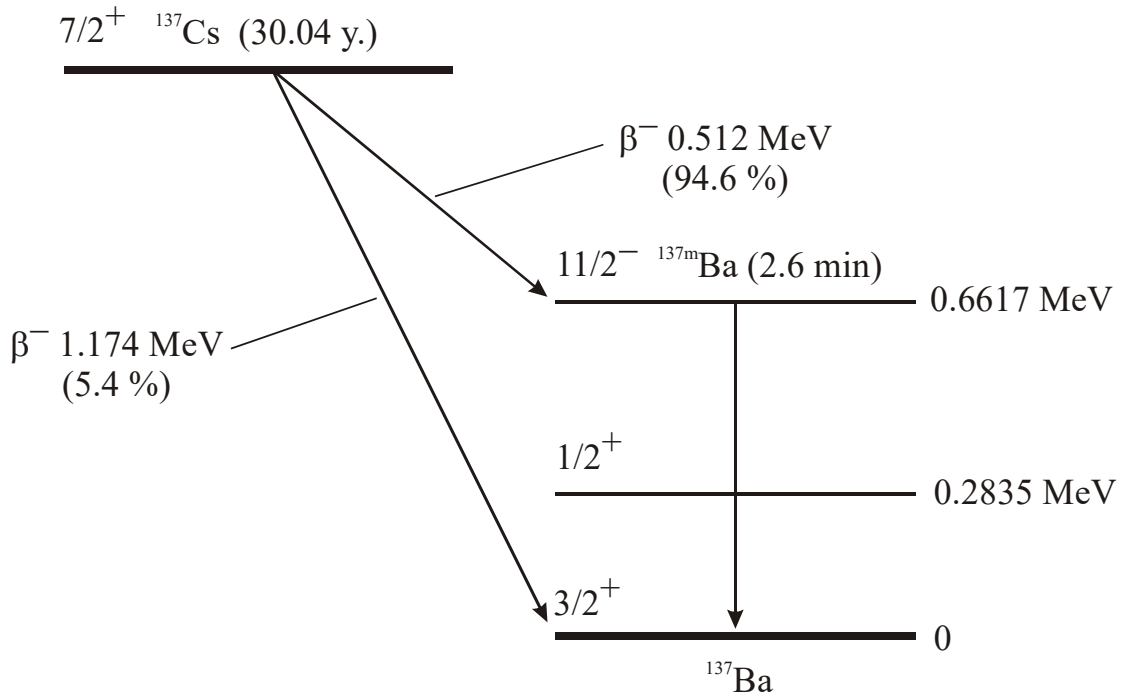


Fig. 16. Decay diagram of ^{137}Cs . This diagram shows the values of the decay half-life, maximum energies of beta particles, probabilities of two beta decay channels, three lowest energy levels of the ^{137}Ba nucleus, and the most likely quantum transition between them.

7. Linear fitting

The aim of linear fitting is determination of the least squares estimates of the coefficients A and B of the linear equation

$$y = A + B \cdot x, \quad (7.1)$$

The essence of the method of least squares is the following. Let us assume that a data set consists of the argument values $x_1, x_2, \dots, x_{n-1}, x_n$ and corresponding values of the function $y(x)$. A typical example is a set of measurement data. In such a case, n is the number of measurements. The measured function values will be denoted y_1, y_2, \dots, y_n . The “theoretical” value of y at a given argument value x_k is a function of the unknown coefficients A and B (see (7.1)), hence we can write $y(x_k) = y(x_k; A, B)$ ($k = 1, 2, \dots, n$). The problem of estimating the coefficients A and B is formulated as follows. The most likely values of A and B are the values that minimize the expression

$$F(A, B) \equiv \sum_{k=1}^n [y(x_k; A, B) - y_k]^2. \quad (7.2)$$

Expression (7.2) is the sum of squared deviations of theoretical values from the measured ones (hence the term “least squares”). This sum is also called “the sum of squared errors” (SSE). This expression always has a minimum at certain values of A and B . However, even if the form of the theoretical function $y(x)$ correctly reflects the true relationship between the measured quantities y and x , those “optimal” values of A and B , which correspond to the minimum SSE, do not necessarily coincide with the true values of A and B (for example, because of measurement errors). The method of least squares only allows estimation of the most likely values of A and B .

Everything that was stated above about the method of least squares also applies to the case when the theoretical function is nonlinear. Regardless of the form of that function and of the number of unknown coefficients, a SSE expression of the type (7.2) must be minimized. However, when $y(x)$ is the linear function (7.1), this problem can be solved analytically (i.e., A and B can be expressed using elementary functions), but when $y(x)$ is nonlinear, this problem can only be solved numerically (applying an iterative procedure).

If $y(x)$ is the linear function (7.1), then the SSE expression (7.2) can be written as follows:

$$F(A, B) \equiv \sum_{k=1}^n (A + Bx_k - y_k)^2 = nA^2 + B^2 \sum_{k=1}^n x_k^2 + \sum_{k=1}^n y_k^2 + 2AB \sum_{k=1}^n x_k - 2A \sum_{k=1}^n y_k - 2B \sum_{k=1}^n x_k y_k. \quad (7.3)$$

It is known that partial derivatives of a function with respect to all arguments at a minimum point are zero. After equating to zero the partial derivatives of the expression (7.3) with respect to A and B , we obtain a system of two linear algebraic equations with unknowns A and B . Its solution is

$$B = \frac{n \sum_{k=1}^n x_k y_k - \left(\sum_{k=1}^n x_k \right) \left(\sum_{k=1}^n y_k \right)}{n \sum_{k=1}^n x_k^2 - \left(\sum_{k=1}^n x_k \right)^2}, \quad (7.4)$$

$$A = \frac{1}{n} \sum_{k=1}^n y_k - \frac{B}{n} \sum_{k=1}^n x_k. \quad (7.5)$$

The B coefficient is called the “slope” of the straight line, and the A coefficient is called the “intercept”. The uncertainties (also called “errors”) of these two coefficients are calculated according to formulas

$$\Delta A = \sqrt{\frac{F_{\min}}{n(n-2)} \left(1 + \frac{\bar{x}^2}{D_x} \right)}, \quad (7.6)$$

$$\Delta B = \sqrt{\frac{F_{\min}}{n(n-2)D_x}}, \quad (7.7)$$

where F_{\min} is the minimum value of the SSE (7.3), i.e., the value of SSE when A and B are equal to their optimal values (7.4) and (7.5), \bar{x} is the average argument value:

$$\bar{x} = \frac{1}{n} \sum_{k=1}^n x_k, \quad (7.8)$$

and D_x is the variance of the argument values:

$$D_x = \frac{1}{n} \sum_{k=1}^n (x_k - \bar{x})^2 = \frac{1}{n} \sum_{k=1}^n x_k^2 - \bar{x}^2. \quad (7.9)$$